Inhibition of "self" engulfment through deactivation of myosin-II at the phagocytic synapse between human cells

Richard K. Tsai[1] and Dennis E. Discher[1,2]

[1]Biophysical Engineering Laboratory, and [2]Cell and Molecular Biology Graduate Group, University of Pennsylvania, Philadelphia, PA 19104

Phagocytosis of foreign cells or particles by macrophages is a rapid process that is inefficient when faced with "self" cells that display CD47—although signaling mechanisms in self-recognition have remained largely unknown. With human macrophages, we show the phagocytic synapse at cell contacts involves a basal level of actin-driven phagocytosis that, in the absence of species-specific CD47 signaling, is made more efficient by phospho-activated myosin. We use "foreign" sheep red blood cells (RBCs) together with CD47-blocked, antibody-opsonized human RBCs in order to visualize synaptic accumulation of phosphotyrosine, paxillin, F-actin, and the major motor isoform, nonmuscle myosin-IIA. When CD47 is functional, the macrophage counter-receptor and phosphatase-activator SIRPα localizes to the synapse, suppressing accumulation of phosphotyrosine and myosin without affecting F-actin. On both RBCs and microbeads, human CD47 potently inhibits phagocytosis as does direct inhibition of myosin. CD47–SIRPα interaction initiates a dephosphorylation cascade directed in part at phosphotyrosine in myosin. A point mutation turns off this motor's contribution to phagocytosis, suggesting that self-recognition inhibits contractile engulfment.

Introduction

A phagocytic cell engulfs another cell or particle that is IgG-opsonized in a coordinated process of adhesion, pseudopod extension, and internalization with phagosome closure. Upon initial binding of IgG, the phagocyte's Fc receptors (FcγRs) activate cytoskeletal assembly with rapid accumulation of phosphopaxillin (Greenberg et al., 1994; Allen and Aderem, 1996) and F-actin (Wang et al., 1984; Greenberg et al., 1991) among other components at a "phagocytic synapse". Nonmuscle myosins also accumulate and suggest a role(s) for contractile motors during particle internalization (Stendahl et al., 1980; Valerius et al., 1981; Diakonova et al., 2002). Signaling activities that influence synapse assembly continue to be clarified (Aderem and Underhill, 1999) and are presumably key to how the macrophage distinguishes foreign cells or particles from autologous cells of "self". Autologous cells are certainly opsonized by Ig (Turrini et al., 1993), and so activation differences are not the complete story. Indeed, based on studies of knockout mice lacking the membrane receptor CD47, this protein on target cells is a phagocytosis-inhibiting "marker of self" (Oldenborg et al., 2000).

CD47 is a ubiquitous member of the Ig superfamily that interacts with the immune inhibitory receptor SIRPα (signal regulatory protein) found on macrophages (Fujioka et al., 1996; Veillette et al., 1998; Jiang et al., 1999). Although CD47–SIRPα interactions appear to de-activate autologous macrophages in mouse, severe reductions of CD47 (perhaps 90%) are found on human blood cells from some Rh genotypes who show little to no evidence of anemia (Mouro-Chanteloup et al., 2003) and also little to no evidence of enhanced cell interactions with phagocytic monocytes (Arndt and Garratty, 2004). Here, we assess the species-specific inhibition of phagocytosis by CD47–SIRPα interactions at the phagocytic synapse and visualize how the interaction affects cytoskeletal activity.

CD47-SIRPα binding is conserved but species-specific (Subramanian et al., 2007). Based on this divergence and assuming an inhibitory role for human CD47, human macrophages might be expected to efficiently phagocytose opsonized sheep red blood cells (RBCs), which is certainly consistent with years of data showing sheep RBCs are readily phagocytosed by human macrophages (Lowry et al., 1998; Botelho et al., 2000; Cooney et al., 2001). We show below that human-CD47 can inhibit

Correspondence to Dennis E. Discher: discher@seas.upenn.edu

Abbreviations used in this paper: DIC, differential interference contrast; NMM, nonmuscle myosin.

The online version of this paper contains supplemental material.

The Journal of Cell Biology, Vol. 180, No. 5, March 10, 2008 989–1003
http://www.jcb.org/cgi/doi/10.1083/jcb.200708043

Fc-receptor mediated phagocytosis by human-derived macrophages and monocytes, but first we map some key components of the phagocytic synapse and identify species-specific differences in localization of SIRPα, phosphotyrosine, and nonmuscle myosin. A microbead system demonstrates the density and affinity dependence of CD47-mediated inhibition and identifies a threshold activity in the inhibitory signaling. These signals propagate downstream and parse cytoskeletal pathways, ultimately implicating a novel phosphotyrosine site on myosin that appears associated with myosin enrichment and contractile function in high efficiency internalization.

Results

Affinity, signaling, and cytoskeleton at the phagocytic synapse with and without CD47

Consistent with recent results showing species-specific CD47–SIRPα interactions (Subramanian et al., 2007), soluble human-SIRPα is found here to bind much less to sheep RBCs than to human RBCs (Fig. 1 A). Both species of RBC are extensively used below in studies of phagocytosis, but in order to eliminate other potential differences between species we also developed avidin-coated microbeads that display recombinant, biotinylated human CD47. These beads demonstrate a moderate affinity and saturable interaction of CD47 for SIRPα and also establish effective blocking of CD47 (B6H12) with a $F(ab')_2$ made from a monoclonal antibody that is known to inhibit SIRPα binding (Fig. 1 B).

To assess the effect of CD47 on protein localization to the phagocytic synapse, we first imaged human-derived THP-1 macrophages incubated with IgG-opsonized human RBCs or sheep RBCs. Briefly, the RBCs were allowed to settle and bind macrophages at 4°C, and then 10 min after warming to 37°C, cells were fixed and immunostained. Imaging by differential interference contrast (DIC) microscopy allowed an unbiased identification of phagocyte–RBC contacts (Fig. 2 A). Subsequent immunofluorescence showed that human-RBCs in contact with the human macrophages stimulated accumulation of SIRPα at the synapse. Such localization was lacking both with sheep RBC and after blocking human RBC with a $F(ab')_2$ of the anti-CD47 (Fig. 1 B inset; Fig. S2, A–C); the removal of the Fc domain ensured no activating signal. Quantitative intensity analyses of randomly chosen synapses showed a fivefold enrichment of SIRPα with human–RBC contacts when compared with either sheep RBCs or CD47-blocked human RBCs (Fig. 2 B, top).

Tyrosine phosphorylation is known to be strongly enhanced when macrophages phagocytose IgG-opsonized targets. Compared with SIRPα, phosphotyrosine showed the opposite trends after immunostaining: synapses with human RBCs showed only a small increase of phosphotyrosine above cytoplasmic levels and at a level that was 3.2-fold lower than sheep RBCs or CD47-blocked human RBCs (Fig. 2 B, bottom). IgG interactions with Fc receptors (FcγRs) are well known to initiate Src family phosphorylation of the immunoreceptor tyrosine-based activating motif (ITAM) that then propagate a phosphorylation cascade (Huang et al., 1992; Ghazizadeh et al., 1994; Greenberg et al., 1994). In contacts with human RBCs, however, the CD47-induced accumulation of SIRPα at the synapse is expected to phospho-activate SIRPα's immunoreceptor tyrosine-based inhibiting motif (ITIM) (Kharitonenkov et al., 1997) with subsequent recruitment of inhibitory tyrosine phosphatases, particularly SHP-1 (Tsuda et al., 1998; Veillette et al., 1998; Vernon-Wilson et al., 2000; Kant et al., 2002). Phosphatase activation is consistent with the relatively large and dominant decrease found here for phosphotyrosine.

Pseudopod extension and phagocytic cup formation around the target predictably requires extensive remodeling of the actin cytoskeleton. Surprisingly, SIRPα–CD47 interactions did not exert any statistically significant effect (P = 0.3) on

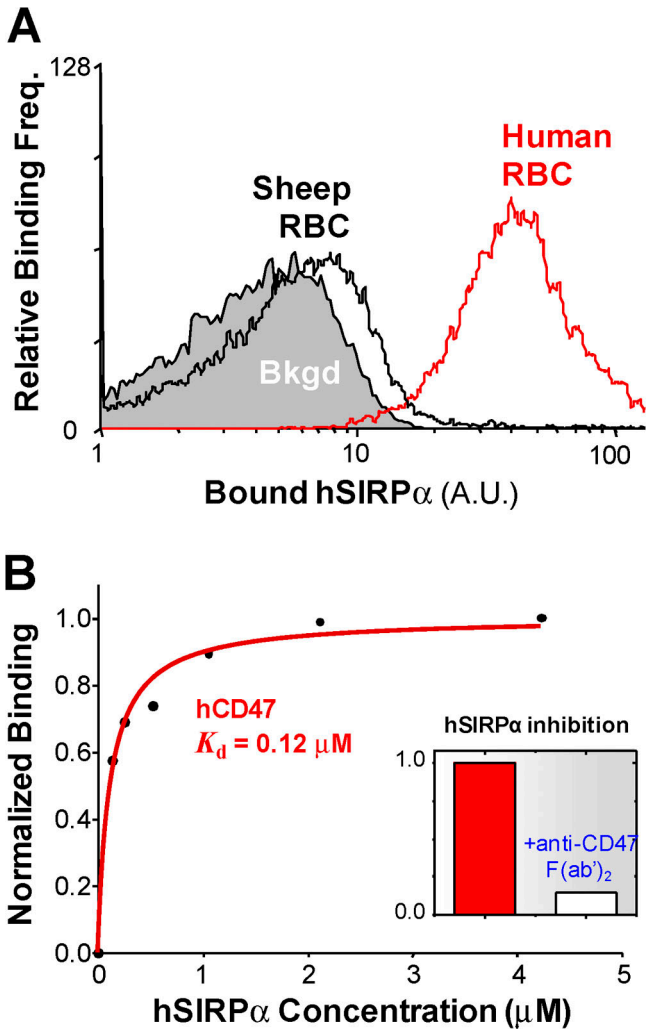

Figure 1. **Species-specific binding of soluble human SIRPα to RBCs and CD47-coated beads.** (A) Fresh human and sheep RBCs binding to soluble hSIRPα (4 μM of GST conjugate), as detected by FITC-anti-GST. "Bkgd" is obtained with RBCs plus antibody. (B) Affinity of hCD47-coated beads binding to soluble hSIRPα based on flow cytometry (see Fig. S2, available at http://www.jcb.org/cgi/content/full/jcb.200708043/DC1). Saturation binding fit gave the indicated dissociation constant, K_d. Because this is a 3D binding constant relevant to binding in a narrow membrane gap between two cells, it is equivalent to $K_d \approx 1$ molecule/[10 nm x (10 μm)^2], which is the concentration of free SIRPα that would half-saturate CD47 on a surface. The inset shows inhibition of soluble hSIRPα binding to hCD47 beads by using anti-CD47 $F(ab')_2$ generated from B6H12 antibody; similar inhibition is obtained with human RBCs.

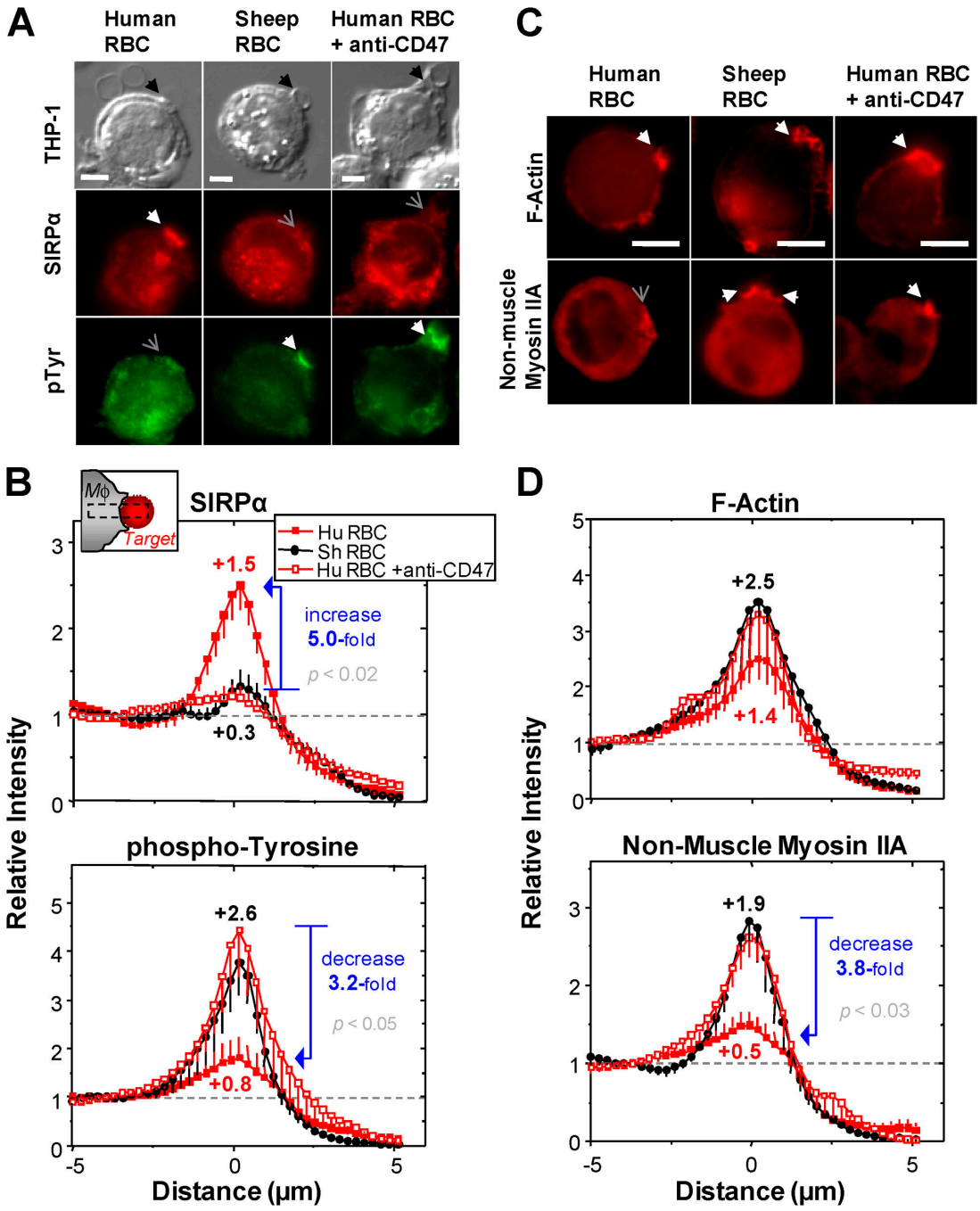

Figure 2. **Signaling and cytoskeletal proteins at the phagocytic synapse depend on CD47.** Human-derived THP-1 macrophages (*Mϕ*) were incubated for 10 min at 37°C with IgG-opsonized human RBCs or sheep RBCs (*Target*: HuRBC or ShRBC) for 10 min. Blocking is done with anti-CD47 $F(ab')_2$. After fixation, cells were stained for SIRPα and pTyr (A and B) or F-actin and nonmuscle myosin IIA (C and D). Phagocytic synapses are indicated with black arrowheads in DIC images, and in fluorescence images with either white or gray arrowheads, depending on enrichment. Bars, 10 μm. Protein localization was quantified for phagocytic synapses randomly selected in DIC images ($n = 5$, ± SD).

F-actin localization to the synapse (Fig. 2, C and D, top). Previous reports have also suggested a role for nonmuscle myosin in phagocytosis (Mansfield et al., 2000), and immunofluorescence for the dominant myosin isoform, nonmuscle myosin IIA (NMM IIA), shows clear recruitment to both sheep RBCs and CD47-blocked human RBCs. However, localization of myosin to the synapse with human RBCs is minimal, with a 3.8-fold decrease relative to sheep RBCs and CD47-blocked human RBCs (Fig. 2, C and D, bottom).

Recruitment of NMM IIA to the synapse formed with sheep RBCs was seen to take minutes and to persist typically for at least 15 min (Fig. 3 A). Macrophages were stably transfected with GFP-NMM IIA, and real-time fluorescence imaging was used to follow the contact and engulfment process. Both sheep RBCs and human RBCs adhered and engaged the macrophages, initiating the formation of a phagocytic cup, but NMM IIA did not enrich adjacent to the human RBCs (Fig. 3, B and C). RBC contacts per macrophage additionally showed no major

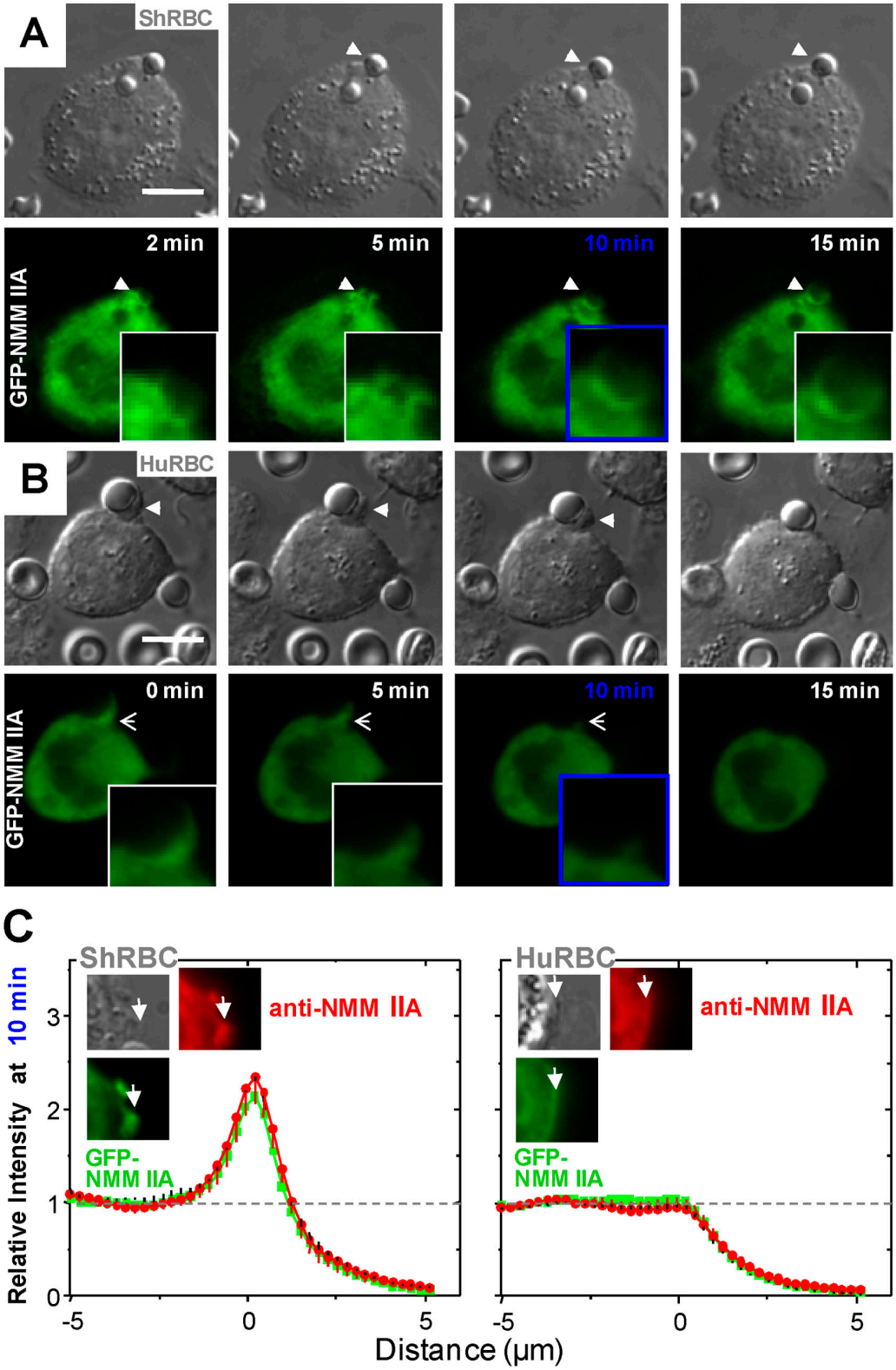

Figure 3. **Time-lapse image of phagocytic synapse formation.** Human-derived THP-1 macrophages stably transfected with GFP-NMM IIA were incubated at 37°C with IgG-opsonized sheep RBCs (A) or human-RBCs (B) for 10 min after an initial 4°C incubation. Time-lapse images in DIC and fluorescence microscopy were taken upon identification of a target cell adhered to the macrophage. Arrows indicate the site of target cell contact with magnified images of the phagocytic synapse. Bars, 10 μm. (C) Phagocytic synapses fixed after 10 min. Cells were immunostained for total NMM IIA and protein localization to the phagocytic synapse was quantified for randomly chosen GFP$^+$ cells by normalization to cytoplasmic intensity of 1.0 (n = 5, ± SD).

difference in adhesion frequency (Fig. S1, available at http://www.jcb.org/cgi/content/full/jcb.200708043/DC1), which is consistent with divergent events subsequent to adhesion.

Myosin recruitment to the phagocytic synapse is inhibited by blebbistatin

Nonmuscle myosin has long been known to be expressed in macrophages (Stendahl et al., 1980), and although recent studies have implicated myosin in FcγR-mediated phagocytosis (Swanson et al., 1999; Titus, 1999; Mansfield et al., 2000; Diakonova et al., 2002) through inhibition studies with 2,3-butanedione monoxime (BDM), this is a relatively nonspecific drug compared with blebbistatin (Ostap, 2002; Limouze et al., 2004). This recently synthesized, membrane-permeable drug inhibits the ATPase activity of myosin types II and VI (Straight et al., 2003; Kovacs et al., 2004). Consistent with a significant role for myosin in phagocytosis, we found that incubation of macrophages with blebbistatin, inhibited enrichment of NMM IIA at synaptic contacts with sheep RBCs targets (Fig. 4, A and B). CD47 on human RBCs induced quantitatively similar effects on NMM IIA. In contrast, F-actin localization to the synapse again appeared statistically the same for sheep RBCs in the presence or absence of the myosin inhibitor as well as for CD47-blocked human RBCs.

Paxillin is also known from past studies to accumulate at the phagocytic synapse (Greenberg et al., 1994) and to be phosphorylated (Hall, 1998). Phospho-paxillin Y^{118} localized to the synapse with sheep RBCs and this persisted with myosin inhibition by blebbistatin (Fig. 4 A). In contrast, human RBCs inhibited phospho-paxillin localization through the effects of CD47. Note the double-labeling studies here consistently show statistically similar levels of F-actin localization, whereas phospho-paxillin varies. Phosphatase activity initiated by CD47–SIRPα interaction likely has multiple downstream targets that directly or indirectly include phospho-paxillin and—as elaborated below—a novel phosphorylation site in myosin.

Phagocytosis increases upon blocking CD47 on human RBCs

Past results from mouse cells certainly suggest that CD47 inhibits phagocytosis, but evidence has been lacking with human phagocytes interacting with any type of target cell or particle. CD47-blocking of human RBCs with the $F(ab')_2$ was shown above to perturb the phagocytic synapse, which made the synapse look like that of sheep RBCs interacting with macrophages (Fig. 2). Human CD47's interaction with SIRPα was certainly blocked (Fig. 1 B inset; Fig. S2, A–C, available at http://www.jcb.org/cgi/content/full/jcb.200708043/DC1), and so we expected that CD47-blocked human RBCs would be engulfed by human phagocytes at a greater frequency than untreated cells.

Phagocytosis by the human-derived THP-1 macrophages of IgG-opsonized RBCs was studied by imaging in DIC microscopy: after 45 min at 37°C the non-engulfed RBCs were hypotonically lysed (Fig. 5 A) and the number of ingested RBCs per macrophage was counted. Phagocytosis by fresh human peripheral blood monocytes used fluorescence to visualize RBCs, all of which had membranes prelabeled with PKH26 (red), and then the non-engulfed RBCs were labeled with a fluorescein-labeled (green) antibody against the Fc of the IgG-opsonin (Fig. 5 B). For either type of human phagocyte, human RBCs were internalized at a small fraction of the frequency of sheep RBCs (Fig. 5, C and D), but a small number of human RBCs was always engulfed for either type of phagocyte. All dependencies on IgG-opsonization fit well to a saturation binding process, consistent with specific activation of the FcR phagocytosis pathway. Most important, blocking of CD47 on human RBCs produced major increases in phagocytosis (blue arrows) with two- to threefold more engulfment that approached or slightly exceeded the phagocytosis of sheep RBCs.

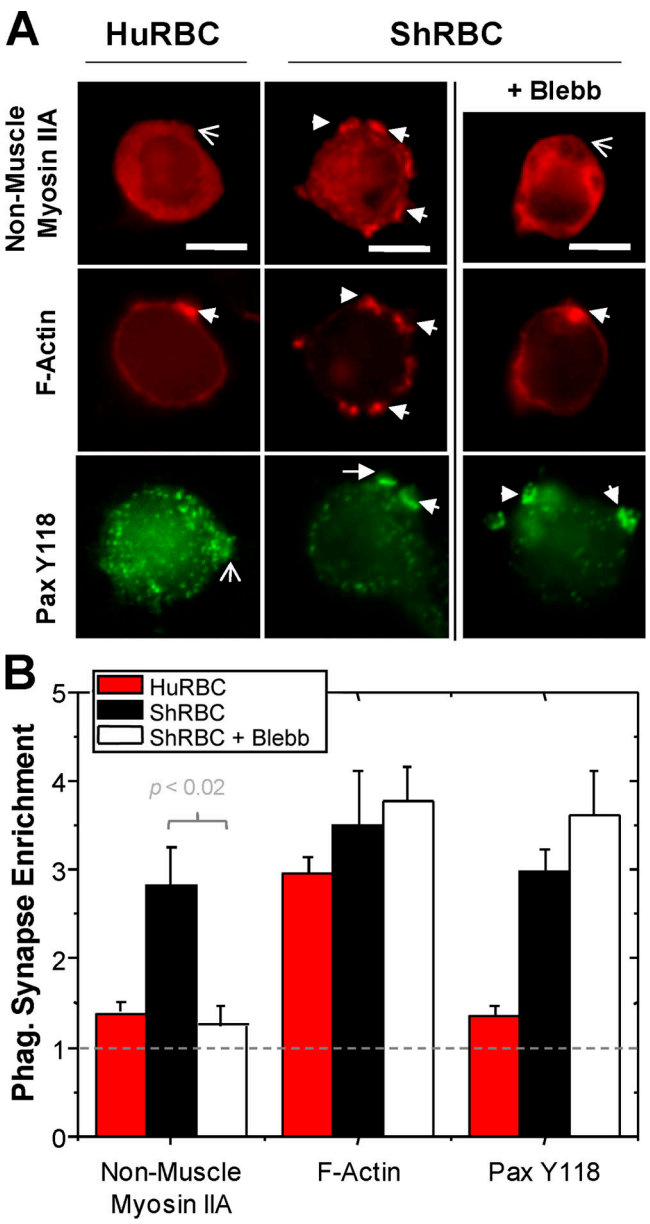

Figure 4. **CD47 inhibits myosin localization similar to blebbistatin.** Phagocytic synapses of THP-1 macrophages with IgG-opsonized sheep or human RBCs (37°C, 10 min) after preincubation with blebbistatin (50 μM, 10 min). DMSO control showed no effect. (A) Cells fixed and immunostained for nonmuscle myosin IIA, F-actin, paxillin-Y^{118}. Bars, 10 μM. (B) Quantitation of protein localization to the phagocytic synapse relative to the cytoplasmic intensity set at 1.0 (n = 5 cells, ± SD).

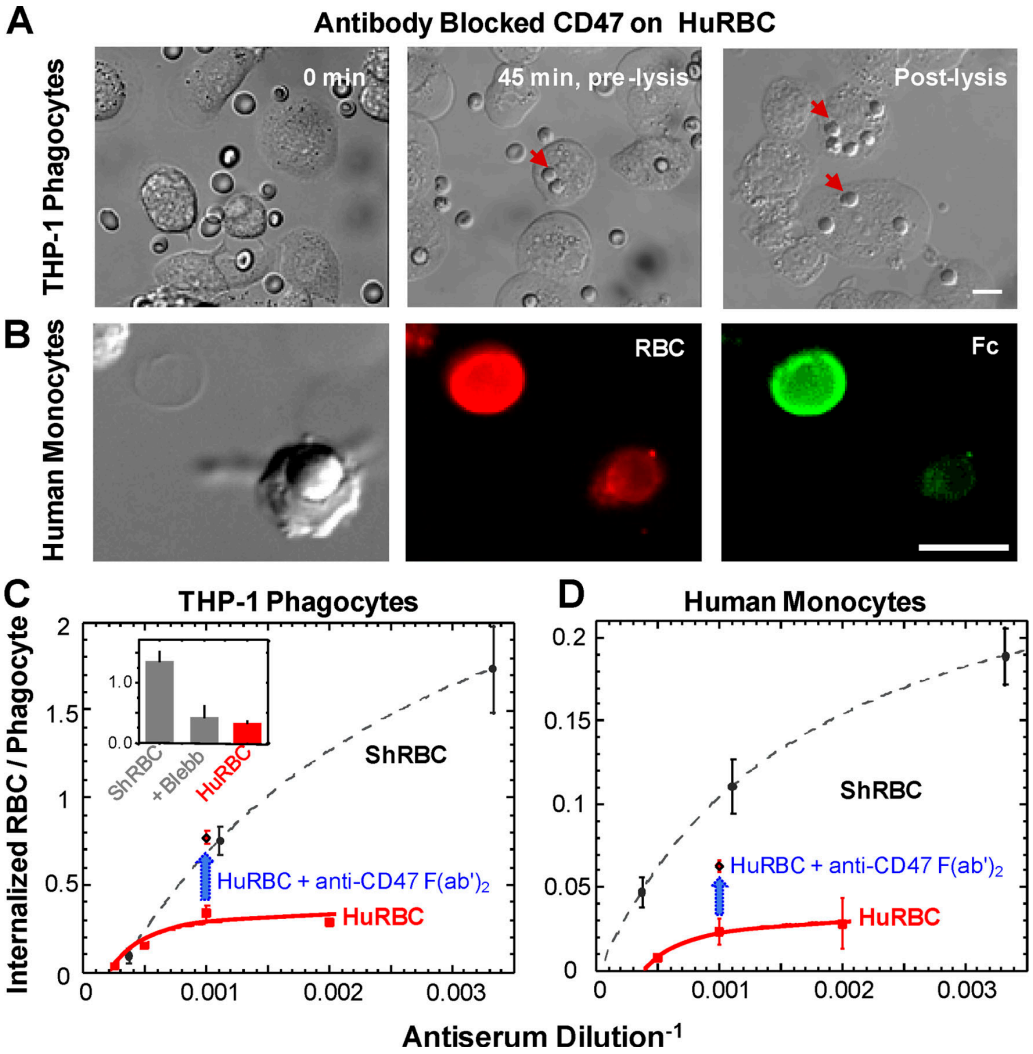

Figure 5. **Human macrophages and monocytes are inhibited by human CD47.** (A) DIC images of THP-1 phagocytes plus CD47-blocked, IgG-opsonized human RBCs, using F(ab')$_2$ made from monoclonal B6H12. 45 min at 37°C is sufficient time for phagocytic internalization of RBCs, which are protected from hypotonic lysis. Bars, 10 mm. (B) Human peripheral blood monocyte plus CD47-blocked human RBCs after lysis, after 45 min of phagocytosis. Red: PKH26-labeled human RBCs. Green: lysed RBCs labeled with FITC-anti-Fc indicating the cell is not internalized. Human RBCs and sheep RBCs were phagocytosed by THP-1 cells (C) or human monocytes (D), showing phagocytosis increases with opsonization. Inset shows blebbistatin treatment of ShRBC showing decrease in phagocytosis. Phagocytosis is measured as the ratio of internalized RBCs per phagocyte, with 200 phagocytes counted in triplicate experiments (± SEM).

Nonmuscle myosin IIA contributes to FcγR-mediated phagocytosis, but is not essential

In light of the myosin differences seen by fluorescence at the various synapses (Figs. 2–4), we also examined the effect of blebbistatin-inhibited myosin on phagocytosis. Engulfment of sheep RBCs by THP-1 macrophages was found to be inhibited by blebbistatin to an extent similar to that of CD47 on human RBCs (Fig. 5 C, inset bar graph). Moreover, a dose–response gave a $K_{\text{i-blebb}} \approx 5$ μM for blebbistatin inhibition of phagocytosis (Fig. S3, available at http://www.jcb.org/cgi/content/full/jcb.200708043/DC1), which is in excellent agreement with the $K_{\text{i-ATPase}}$ for inhibition of NMM IIA's ATPase by blebbistatin (Limouze et al., 2004).

To directly confirm the implied correlation between synaptic myosin and the extent of phagocytosis, fluorescence imaging was repeated on the enrichment of myosin and F-actin at the synapse for both human and sheep RBCs treated with or without blebbistatin. As demonstrated in Figs. 4 and 5, when synaptic NMM IIA is at or near background cytoplasmic levels, phagocytosis is low but nonzero. The comparatively rapid enrichment of F-actin at the phagocytic synapse described here and by others (Strzelecka et al., 1997) proved here to be dependent primarily on the initial synaptic contact rather than the ultimate level of phagocytosis. The result highlights a basal level of pseudopod extension and engulfment that is independent of myosin.

CD47 on microbeads is sufficient to inhibit phagocytosis

RBCs are common targets in phagocytosis, but RBC membranes are complex and blocking results above could have other interpretations. We therefore tested whether CD47 alone on synthetic microbeads could also inhibit phagocytosis. The extracellular immunoglobulin-like domains of human CD47 (hCD47) was recombinantly expressed with a spacer domain

(Brown and Barclay, 1994; Brown et al., 1998) plus a C-terminal biotinylation site. Biotinylation allowed attachment of soluble hCD47 to streptavidin-coated beads (2.1 μm) (Fig. 6 A, schematic), with density adjustable to levels previously measured for normal and diseased RBCs (Dahl et al., 2004; Subramanian et al., 2006).

To study phagocytosis, beads (Fig. 6 A, red) were opsonized by pretreatment with anti-streptavidin to again induce FcR-mediated phagocytosis (for 45 min at 37°C); and non-engulfed beads were detected with a flourescein anti-Fc (green) against the IgG-opsonin. The number of adherent IgG-opsonized beads per phagocyte was independent of hCD47 (Fig. S1). As mentioned in the previous RBC studies (Fig. 5 B), phagocytosed beads were sterically protected so that the merged DIC and fluorescent images provided a definitive means to quantify the internalized beads per phagocyte.

The phagocytosis results for beads proved wholly consistent with the RBC results. With increasing opsonization and for both THP-1 cells and the human monocytes, the uncoated "CD47-null" beads were phagocytosed more than beads displaying hCD47 (Fig. 6 B). The dependence on the level of IgG-opsonization fit well to a saturation binding process, consistent again with the specificity of FcR-activated phagocytosis (also see RBC results, Fig. 5, C and D). Likewise, blebbistatin inhibited phagocytosis of CD47-null beads to a level similar as hCD47 beads and again yielded a $K_{\text{i-blebb}}$ consistent with inhibition of NMM IIA's ATPase (Fig. S3), confirming once again the role of nonmuscle myosin. Furthermore, blocking CD47 on hCD47 beads again produced an increase in phagocytosis, demonstrating that the Ig domain of human CD47 is sufficient to inhibit phagocytosis.

Density dependence of CD47 in species-specific inhibition of phagocytosis

Studies of knockout mice have implicated CD47 as a marker of self on mouse RBCs (Oldenborg et al., 2000); however, humans with major co-deficiencies of CD47 on their RBCs show no evidence of enhanced phagocytic interactions (Mouro-Chanteloup et al., 2003; Arndt and Garratty, 2004). Known and unknown differences between RBCs from different species also motivate a common phagocytic target. We therefore sought to use the hCD47-coated microbeads (see Fig. 1) and establish the inhibitory density dependence of hCD47 with a common IgG opsonin. These two ligands, hCD47 and IgG, do not compete and do not interfere with SIRPα binding (Fig. S2 D).

Beads were opsonized at saturating densities of IgG (Fig. 6 B) and then, over a 20-fold range of CD47 densities, the number of internalized beads per THP-1 was measured (Fig. 6 C). Human-CD47 gave a K_i at high opsonin of 20 CD47/μm^2, which appears ~10-fold less than normal human RBC densities of CD47. Human peripheral blood monocytes interacting with beads bearing high densities of hCD47 showed a similarly potent reduction in phagocytosis (Fig. 6 D). A higher baseline level of bead phagocytosis versus RBCs could reflect the fact that stiffer targets are more readily engulfed (Beningo et al., 2002). More importantly, the results here showed that even 10–20% of normal CD47 densities are sufficient to inhibit phagocytosis.

In the absence of functional CD47, phagocytosis is proportional to myosin

Blebbistatin's inhibition of phagocytosis functionally implicated NMM II because it inhibits all three isoforms (A–C), and so to more directly assess the function of the IIA isoform, the effects of both knockdown and overexpression were functionally studied. Transfection of GFP-NMM IIA added ~50% more total IIA isoform, based on an immunoblot comparison to wild type (Fig. S4, available at http://www.jcb.org/cgi/content/full/jcb.200708043/DC1), and the overexpression also resulted in ~50% more phagocytosis of sheep RBCs (Fig. 7). Similarly, knockdown of NMM IIA with Lentivirus gave ~50% less myosin, and this resulted in nearly 50% less phagocytosis. Transfection of GFP-NMM IIA into the knockdown cells (driven by a powerful CMV promoter) returned expression to near wild-type levels, and also recovered full phagocytic function. Additionally, the GFP-NMM IIA was inhibited ~50% by 5 μM blebbistatin (Fig. 7, inset), which again indicates that this chimeric construct has normal, myosin-like activity. A linear fit ($R^2 = 0.99$) through all of these phagocytosis results for sheep RBCs not only emphasizes the proportional role for myosin in efficient engulfment, but also yields a nonzero intercept at "zero" myosin activity that is nearly the same as the low rate for "actin only" engulfment of human RBCs (~0.2–0.3 RBC per macrophage). These results thus suggest that human CD47 parses pathways and primarily signals inhibition of NMM IIA's contribution to efficient phagocytosis.

CD47 signals through SIRPα and ultimately to myosin

SIRPα localization to the phagocytic synapse with targets presenting CD47 (Fig. 2, A and B) is consistent with ligand-receptor interactions as well as SIRPα ITIM activation and subsequent SHP-1 phosphatase induction (Brown and Frazier, 2001; Latour et al., 2001). Immunoprecipitation of SIRPα followed by Western blot analysis of phosphotyrosine showed a clear and saturable signaling difference with hCD47 (Fig. 8 A). The term denoted as K_i is defined as the normalization of CD47 densities to the phagocytosis inhibition constant for human CD47 (Fig. 6 C) and normalization of phosphotyrosine levels to SIRPα intensities gave an effective signaling constant K_s that approximated the K_i.

CD47's activation of SIRPα (about twofold here) and downstream phosphatase activity is certainly known but downstream phospho-targets have not yet been identified. Studies of SIRPα-knockout macrophages engulfing IgG-opsonized mouse RBCs (Okazawa et al., 2005) suggested no major perturbation of either phospho-FcγR, downstream phospho-Syk or phospho-Cbl, although it had been reported that SHP-1 can dephosphorylate Cbl and thereby moderate Rac activity in FcγR-mediated phagocytosis (Kant et al., 2002). Through immunoblotting, changes in the phosphorylation state of these activator/effector proteins ranged from 1.1- (FcγR) to 1.5-fold (Cbl) (Fig. 8 B). Considerably larger down-regulation of phosphotyrosine by CD47 at the synapse (3.2-fold) was clear in our imaging studies (Fig. 2 B) as was CD47-induced delocalization of myosin and phospho-paxillin (3.8- and 3.0-fold, respectively; Fig. 2 D, Fig. 4 B).

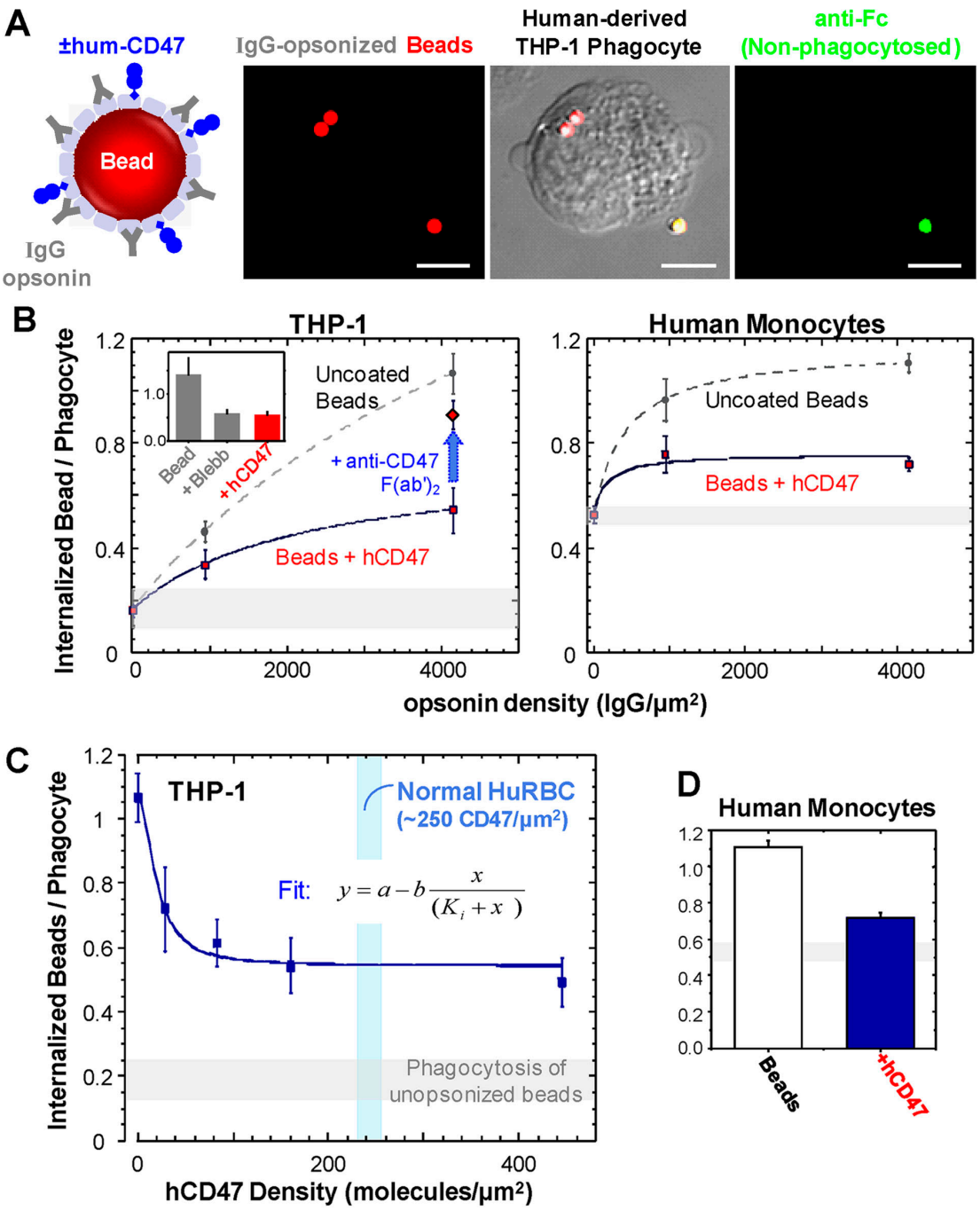

Figure 6. **Human-CD47 is sufficient to inhibit phagocytosis.** (A) Streptavidin beads coated with both anti-streptavidin IgG as the opsonin and biotinylated human CD47. Phagocytosis of beads (red) by THP-1 cells was assessed in DIC and fluorescence microscopy with non-ingested beads (green) visible with rabbit anti-streptavidin plus a second, goat anti–rabbit antibody. Bars, 10 μm. Beads ± hCD47 (at normal RBC density) were engulfed by THP-1 cells or human monocytes (B), demonstrating inhibition of phagocytosis by hCD47 unless the beads are blocked with anti-CD47. Inset bar graph compares to inhibited phagocytosis of uncoated beads after 10 min pretreatment of THP-1 cells with blebbistatin (50 μM). (C) Inhibition of phagocytosis depends on density of human CD47 on beads. All assays were conducted and analyzed as in Fig. 5. Phagocytosis inhibition occurs with an effective $K_i \approx 20$ molecules/μm^2, which considerably exceeds the relevant dissociation constant for a 10-nm gap of $K_{d,10\ nm} \approx 1$ molecule/(10 μm)^2 (Fig. 1 B). This ratio of ~1,000 as well as the known cell surface densities imply that almost all SIRPα and CD47 that diffuse into the gap will bind and thus enrich in the synapse (see Fig. 2, A and B). (D) Bar graph compares hCD47 inhibition of phagocytosis in peripheral blood monocytes.

The only report of phosphotyrosine regulation of NMM IIA suggests it to be a direct target of SHP-1 in B-cells (Baba et al., 2003), with the speculated site of interaction appearing in the N-terminal head domain. Phosphotyrosine regulation of NMM IIA therefore seemed an intriguing possibility to pursue in the present context of CD47 function. Anti-phosphotyrosine immunoblots were made from whole cell lysates of THP-1 cells phagocytosing opsonized human or sheep RBCs (Fig. 8 C). Three band regions (a, b, c) showed the greatest differences in phosphotyrosine levels compared with THP-1 cells alone. Bands a–c each

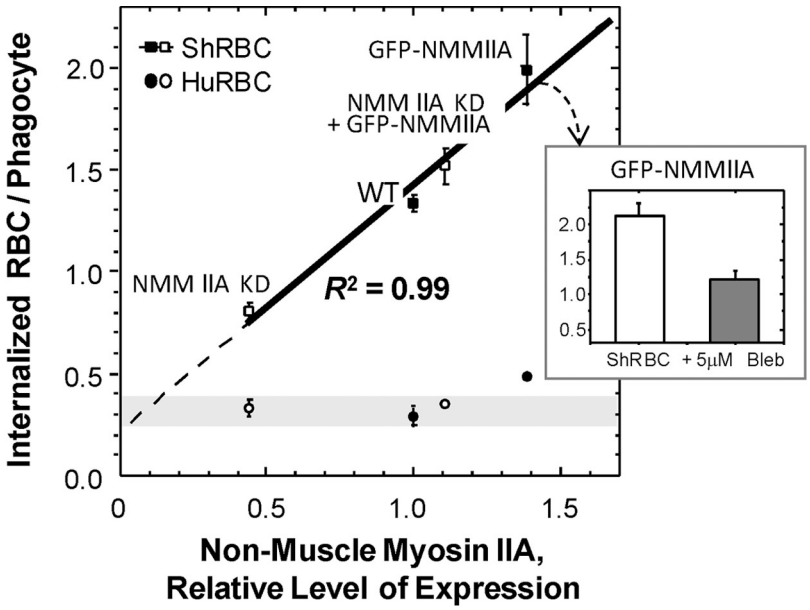

Figure 7. **Myosin increases the efficiency of phagocytosis.** Phagocytosis of IgG-opsonized sheep RBCs was measured as a ratio of internalized RBCs per phagocyte, with 200 phagocytes counted in triplicate experiments (± SEM). The level of NMM IIA activity is normalized to wild-type levels in THP-1, with relative levels of knockdown or overexpression quantified by immunofluorescence and Western blot. Results for phagocytosis of the IgG-opsonized sheep RBCs were fit very well to a line; the intercept approximates the result for human RBCs. Inset bar graph shows blebbistatin inhibition of ShRBC phagocytosis by GFP-NMM IIA expressing wild-type THP-1. No compensating changes in NMM IIB were evident (see Fig. S4 B, available at http://www.jcb.org/cgi/content/full/jcb.200708043/DC1).

showed 3.3- to 1.6-fold less phosphotyrosine with human RBCs versus sheep RBCs (Fig. 8 C, plot), which was similar in range to the down-regulation of phosphotyrosine imaged at the phagocytic synapse (3.2-fold in Fig. 2 B). In fact, band "a" had a MW in the range of nonmuscle myosins in addition to a similarly high level of down-regulation.

To identify the major phosphotyrosine bands a–c, these bands were excised from Coomassie-stained polyacrylamide gels, digested in-gel by trypsin, and the peptide fragments were characterized by liquid chromatography-mass spectrometry/mass spectrometry (LC-MS/MS) (Fig. 8 C). Within band "a", 45 tryptic peptides matched sequences of NMM IIA (23% coverage), including one fragment from myosin's self-assembling tail region with a novel phosphorylation at Y^{1805} (Fig. 8 C, bottom). Additional cytoskeletal proteins that were detected in the macrophages and might be targeted in the CD47-SIRPα phosphotyrosine pathway include Talin-1 (Turner et al., 1989; Greenberg et al., 1990), mDIA1 (Meng et al., 2004), and α-actinin (Crowley and Horwitz, 1995; Izaguirre et al., 1999). Capabilities of MS to identify phosphotyrosine are currently limited, as here, by low sequence coverage and sub-stoichiometric phosphorylation (McLachlin and Chait, 2001). However, the one solid lead from MS of the phosphotyrosine in NMM IIA was first followed up by immunoprecipitation of NMM IIA from the THP-1 lysates and subsequent immunoblotting for phosphotyrosine. The results confirmed the presence of phosphotyrosine in NMM IIA that is ultimately regulated by CD47 interactions (Fig. 8 D).

Phosphotyrosine activation of NMM IIA in phagocytosis

In light of the proportionality between phagocytosis and myosin expression (Fig. 7), several mutants of the GFP-NMM IIA construct were made and studied in their effects on phagocytosis of sheep RBCs and localization to the synapse. One mutant truncated the C terminus by 170 residues and had been found previously to compromise myosin filament assembly and function (Wei and Adelstein, 2000). Two Y→F point mutations were made at the putative phospho-sites in the head (Y^{277}) and tail (Y^{1805}). Although the wild-type GFP-NMM IIA construct showed gain-of-function phagocytosis that was statistically distinct from untransfected wild type ($P < 0.03$), all three mutants appeared the same as wild type (Fig. 9 A). Similar results with even greater statistical significance ($P < 0.01$) were found upon transfection of these constructs into the knockdown macrophages (Fig. 9 A).

Consistent with the lack of a functional contribution to phagocytosis, the GFP mutants exhibited no significant localization to the synapse (Fig. 9 B). Conveniently, the transfections of these GFP constructs into wild-type macrophages also allowed immunostaining for total NMM IIA. Quantitative ratio imaging (see Fig. 2) showed that the endogenous myosin accumulated at phagocytic synapses, whereas the mutant constructs did not. These results contrast with the clear localization of the wild-type GFP-NMM IIA to the phagocytic synapse (Fig. 3 A) and point to the role for phospho-regulation of myosin-II in phagocytosis.

Discussion

Human CD47 has been shown here to communicate marker of self signals to human primary and immortalized monocytes/macrophages, and the mechanism for species-specific inhibition of phagocytosis shows that CD47 parses pathways by selectively down-regulating the cytoskeleton's contractile contributions to engulfment. Our results were obtained with IgG-opsonized RBCs from various species that are common in phagocytosis studies (e.g., sheep RBCs) and also with synthetic beads bearing recombinant CD47. The signaling and remodeling processes are highlighted in Fig. 10. IgG activation of the Fcγ receptor on the phagocytes (Cambier, 1995) is known to induce actin cytoskeleton assembly (Araki et al., 1996;

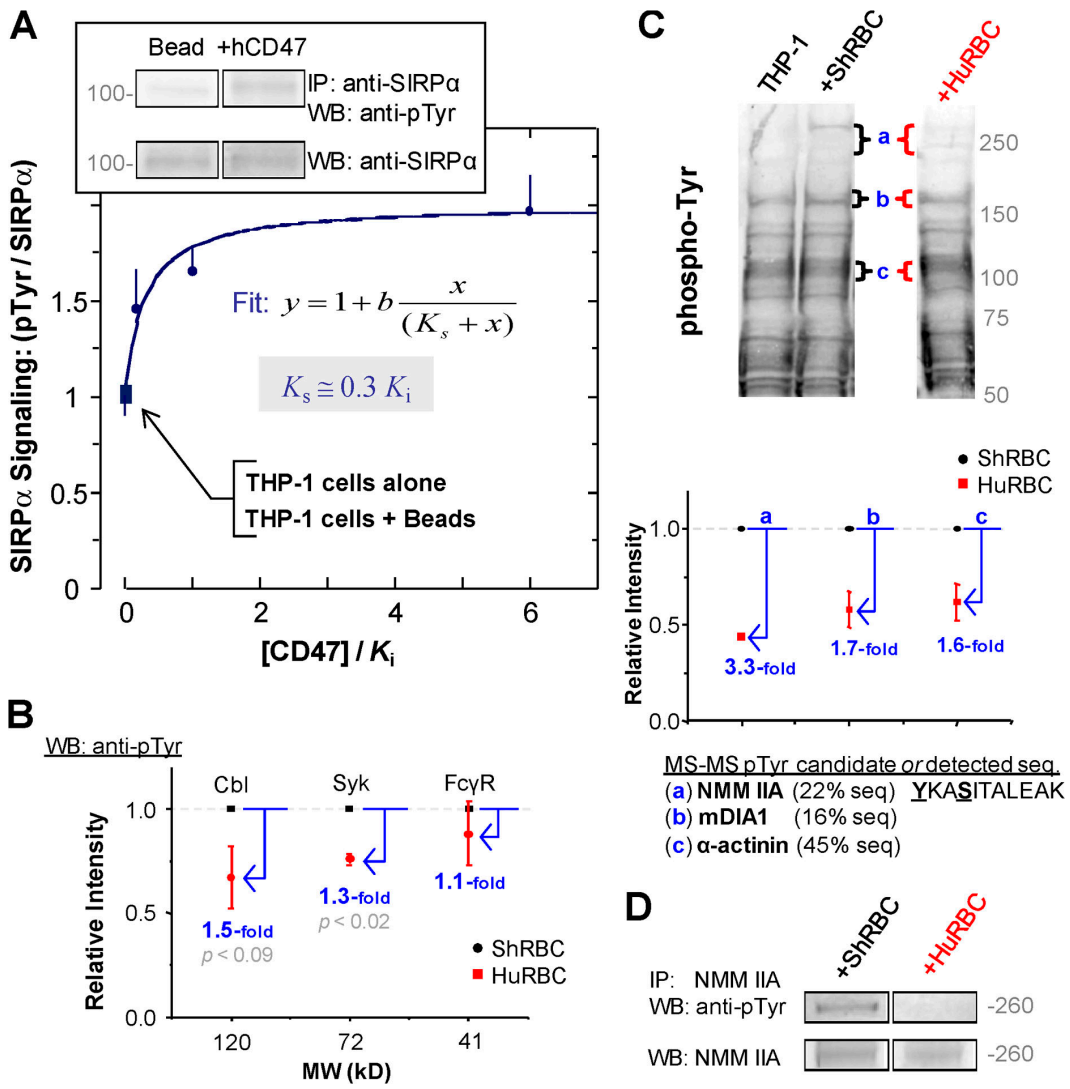

Figure 8. **Species-specific signaling through SIRPα and ultimately to cytoskeletal proteins.** (A) hCD47 was bound at varying densities to opsonized beads and phagocytosed by THP-1 macrophages. From macrophage lysates, SIRPα was immunoprecipitated and immunoblotted (inset) for quantitation of phosphotyrosine and total SIRPα for normalization. Fits of the data gave an effective signaling constant K_s for each species that depends on the CD47 density; all densities are scaled by hCD47's inhibitory constant (K_i) as determined in Fig. 6 at the same opsonization. (B) Phosphotyrosine decreases in Cbl, Syk, and FcγR within THP-1 during phagocytosis of IgG-opsonized human RBCs normalized to sheep RBCs. Whole-cell lysates were immunoblotted and densitometry was used to quantify suitable MW bands (also see Fig. S5, available at http://www.jcb.org/cgi/content/full/jcb.200708043/DC1). (C) Major phosphotyrosine differences in THP-1 during phagocytosis of IgG-opsonized human RBCs versus sheep RBCs. Whole-cell lysates were immunoblotted and densitometry was used to identify bands (a–c) that showed the largest relative differences in intensity for sheep or human RBC targets compared with THP-1 cells. For bands a–c, the plot shows the intensity obtained with phagocytosis of human RBCs relative to sheep RBCs. (triplicate experiments ± SEM). The list from MS analyses of bands a–c indicates top candidate phospho-proteins or else a directly detected sequence (for myosin). (D) Immunoprecipitation of NMM IIA from lysates followed by immunoblot for pTyr, confirming the major decrease in phosphotyrosine NMM IIA when THP-1 phagocytose human RBCs compared with sheep RBCs.

Crowley et al., 1997; Caron and Hall, 1998; Lowry et al., 1998; May and Machesky, 2001), and this F-actin assembly was proven here to be independent of CD47's signaling pathway(s) (Fig. 2). In the absence of CD47 on the target, paxillin assembles at the phagocytic synapse, consistent with past results for IgG-opsonized sheep RBCs (Greenberg et al., 1994; Coppolino et al., 2001), and so does NMM IIA. By contrast, human RBCs with functional CD47 show strong localization of the counter-receptor SIRPα to the synapse (fivefold), and also show strongly reduced levels of both phosphotyrosine and NMM IIA (3.2- and 3.8-fold, respectively; Fig. 2). We find that human CD47 and the myosin inhibitor blebbistatin block synaptic localization of NMM IIA and phagocytosis to the same extent (Fig. 4 B, Fig. 5 C). The proportionality between NMM IIA levels and efficient phagocytosis is also clear from knockdown and overexpression studies (Fig. 7). Although CD47 signals locally, we conclude that it ultimately has a similar, but downstream effect in inhibiting the major myosin isoform's contractile contributions to engulfment.

CD47 in mouse has been described as a marker of self that can inhibit phagocytosis by mouse macrophages (Oldenborg et al., 2000; Gardai et al., 2005). Blocking of CD47 on human RBCs with an anti-CD47 $F(ab')_2$ increased uptake by both human macrophages and monocytes. Given the low densities of

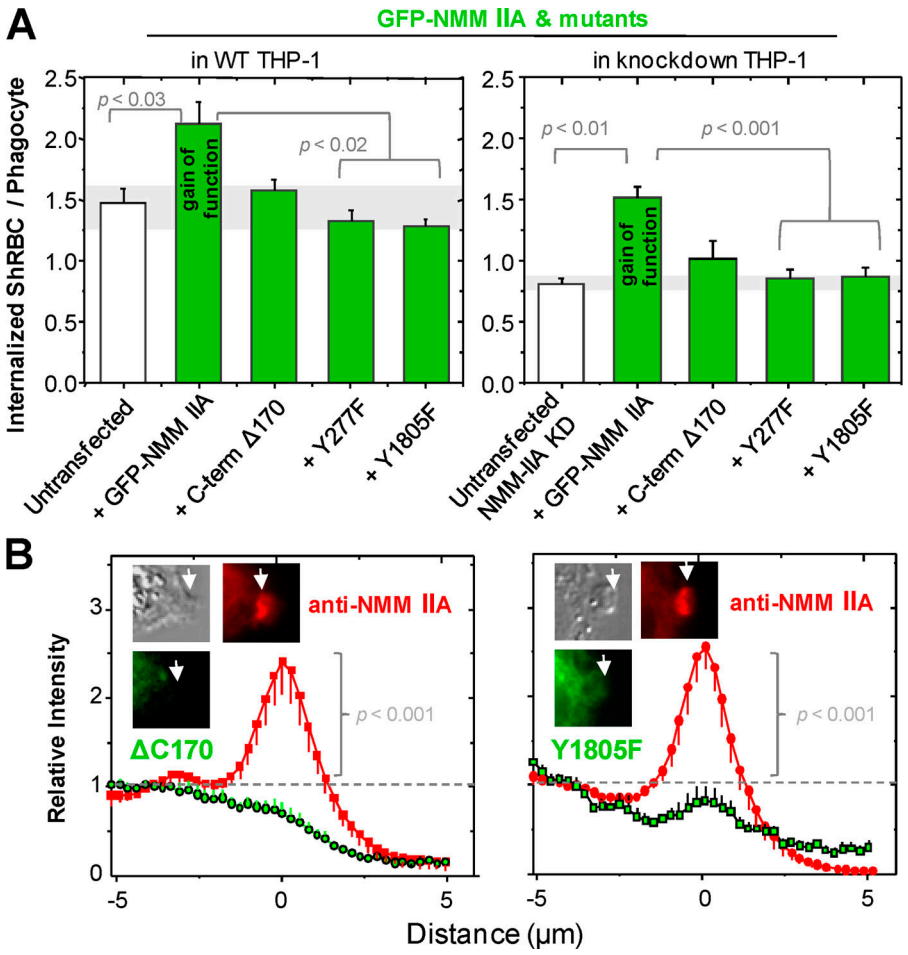

Figure 9. **Phosphorylated myosin IIA important for efficient phagocytosis.** THP-1 macrophages and NMM IIA knockdown THP-1 were used as is or else transfected with GFP-NMM IIA, GFP-ΔC170, GFP-Y277F, or GFP-Y1805F. (A) Phagocytosis of IgG-opsonized sheep RBCs at 37°C for 45 min, measured as the ratio of internalized RBCs per phagocyte with 200 phagocytes counted in triplicate experiments (± SEM). (B) Phagocytic synapses fixed after 10 min. Cells were stained for NMM IIA and protein localization to the phagocytic synapse was quantified for randomly chosen GFP + cells by normalization to cytoplasmic intensity of 1.0 (n = 5, ± SD).

CD47 on cells, this ubiquitous membrane protein seems less likely to mediate cell adhesion than function as an extremely potent signaling receptor, functional at densities of a just a few dozen molecules per μm^2 (Fig. 6 C). Major co-deficiencies of CD47 on human cells (Mouro-Chanteloup et al., 2003) can therefore be tolerated without compromising marker of self function, and because CD47-null humans have yet to be reported, our results suggest an important role for CD47 in the innate immunity of humans.

Regardless of species, normal macrophages should be expected to engulf "self" cells at a considerably lower frequency than typical targets—apoptotic and foreign cells or particles. The decision of a macrophage to phagocytose is in part made by the extent of target opsonization, which activates assembly of the F-actin cytoskeleton at the phagocytic synapse; however, Ig is high in bodily fluids and almost certainly binds or adsorbs at some level to all cells (Turrini et al., 1993), and so activating signals seem unavoidable. CD47 signaling probably occurs in parallel because IgG binding to FcγR (Duchemin et al., 1994) promotes intimate adhesion and thereby promotes hCD47 interactions with SIRPα within the synapse (Fig. 2 A). It will be interesting to visualize the effects of SIRPα polymorphisms in human (as well as mouse) that have been recently described (Takenaka et al., 2007).

Synaptic activation of SHP-1 phosphatase by CD47-SIRPα has been clear, but downstream targets and mechanisms in phagocytosis inhibition have remained unknown. Deactivation could have been restricted to membrane receptors, particularly FcγR, but our phosphorylation data indicates otherwise (Fig. 8). Conceivably, F-actin could have been found to be the primary target of CD47's signaling to macrophages because polymerization alone is sufficient to drive pseudopod extension and particle internalization (May and Machesky, 2001). We find, however, that F-actin establishes a basal level of phagocytosis regardless of CD47. From our sheep versus human comparison of phosphotyrosine and MS analysis of dephosphorylated proteins, NMM IIA emerged as the major down-regulated species (3.3-fold) (Fig. 8 C). This regulation of the myosin heavy chain differs from the usual regulation through the light chain (Conti and Adelstein, 2008). Talin, α-actinin, and the actin nucleator mDia1 also appeared regulated (to a lesser extent), and all have been implicated previously in phagocytosis (respectively: [(Turner et al., 1989; Greenberg et al., 1990); (Crowley and Horwitz, 1995; Izaguirre et al., 1999); (Meng et al., 2004; Brandt et al., 2007)]). Although phospho-paxillin was down-regulated in our imaging studies, it was not prominent in our immunoblots and was unaffected by blebbistatin, which otherwise mimicked CD47's inhibitory effects (Figs. 5 C and 6 B, insets). Nonetheless, focal adhesion-type cytoskeletal assemblies of paxillin, talin (Niewohner et al., 1997), or even α-actinin (Sampath et al., 1998) could also contribute to CD47 function, as these phospho-proteins are also implicated in phagocytosis.

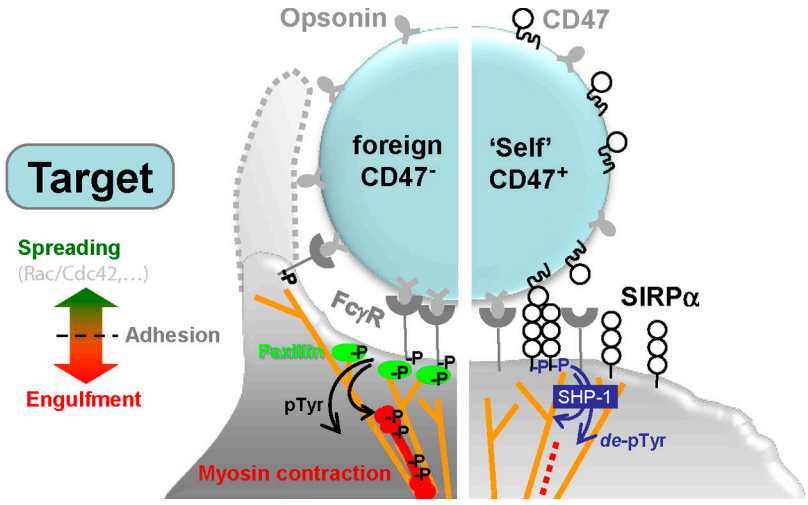

Figure 10. **Phagocytic synapse and CD47's signaling in cytoskeleton remodeling.** IgG-opsonized target cell or particle lacking CD47 results binds FcγR which activates assembly of paxillin, F-actin, and nonmuscle myosin IIA at the synapse. In contrast, parallel interactions with CD47 signals through SIRPα to inhibit myosin assembly and contractile contributions to efficient phagocytosis.

FcγR-induced tyrosine phosphorylation leads to the downstream activation of Rac/Cdc42 (Olazabal et al., 2002), which then signals the recruitment and assembly of F-actin and a focal adhesion type of structure. Syk is not required because macrophages from Syk-deficient mice will extend actin-rich pseudopods around target particles even though FcγR-mediated phagocytosis is ultimately defective (Crowley et al., 1997). In comparison, SIRPα-null macrophages engulf IgG-opsonized mouse RBCs more readily than wild-type macrophages (Okazawa et al., 2005) and show no major differences in either phospho-FcγR, or downstream phospho-Syk or phosho-Cbl. Likewise, in our phagocytosis studies of human versus sheep RBCs, no significant difference in phospho-FcγR was detected, and, relative to phospho-SIRPα and cytoskeletal changes (Fig. 8 C), only small decreases in phospho-Syk or phospho-Cbl were detected (Fig. 8 B: 1.3- and 1.5-fold, respectively). Such differences upstream could in principle reflect a classical amplification of signaling, but our finding of slight decreases in phospho-Cbl due to CD47 is perhaps most consistent with the activity of SHP-1 (Kant et al., 2002). The small effect would suggest perturbations to actin assembly; indeed, with CD47–SIRPα interactions (Fig. 2 D and Fig. 4 B) all suggest a slight tendency toward decreased actin polymerization (based on staining with rhodamine-phalloidin), but the effects on myosin are statistically certain in comparison.

Past studies of antibody-opsonized beads as targets have shown that FcγR-mediated phagocytosis is independent of Rho or ROCK activity while dependent on myosin-II for particle internalization but not for actin cup formation (Olazabal et al., 2002). With CD47 on the target, activation of the SIRPα→SHP-1 phosphatase pathway (Vernon-Wilson et al., 2000) could in principle block engulfment by regulating various kinase or phosphatase activities (such as Cbl) or perhaps even by regulating signaling to NMM IIA. Our immunoblot analysis followed by LC-MS/MS indeed identified direct phosphorylation of Y^{1805} in this myosin's self-assembling tail as an ultimate target for CD47-SIRPα interaction. Mutation of this site disables this major myosin from contributing to phagocytosis (Fig. 9). Moreover, initial studies of NMM IIA in primary human mesenchymal stem cells (that are also marrow derived) identify the same site as being phosphorylated (unpublished data), and since we have shown NMM's contribute in key ways to differentiation of these adult stem cells (Engler et al., 2006), a general mechanism of regulation is perhaps emerging. Detailed study of purified point mutants would certainly help clarify broader effects on myosin assembly/activity, but regulatory roles for specific residues in the myosin tail region already appear reasonable because: (1) nearby sequences (aa 1666–1728 and 1914–1961) are involved in isoform-specific assembly of functional myosin filaments (Sato et al., 2007), and (2) disease-causing mutations occur nearby with the charge changes E1841K and R1933X (Heath et al., 2001). The head and tail of at least some myosin-IIs can interact to form a compact, diffusible monomer and regulatory interactions then open up this conformation for polymerization into filaments (Kudryashov et al., 2002); pY might regulate such a conformational switch. The only other report of a phosphotyrosine in NMM IIA suggested pY^{277} is a direct target for SHP-1 (Baba et al., 2003).

Both phosphotyrosine sites identified here in human myosin are found in mouse, for which CD47's "self" signaling was first described (Oldenborg et al., 2000). Both phospho-sites in NMM IIA are found in other mammalian species as well as in other proteins (i.e., eight myosin heavy chain proteins share the head motif and one non-myosin, coiled-coil protein has the tail motif). In addition, the MS data here indicated that NMM IIA dominates the B and C myosin isoforms by at least 10-fold (Table S1, available at http://www.jcb.org/cgi/content/full/jcb.200708043/DC1), and mouse knockouts of the B and C isoforms do not exhibit immune defects whereas the NMM IIA-null mouse is embryonic lethal as an undifferentiated mass of cells (Conti et al., 2004). The results here with human cells have implicated NMM IIA for good reason it seems and thus suggest that recognition of "self" entails blocking engulfment by turning off this ubiquitous and essential motor.

Materials and methods

Chemicals

Dulbecco's phosphate-buffered saline (DPBS) without Ca^{2+} or Mg^{2+} (Invitrogen) was supplemented with either 1% BSA or 1% BSA + 0.05% Tween 20 (Sigma-Aldrich). PKH26 (Sigma-Aldrich) hydrophobic dye was used for

red cell labeling. TBS (Tris-buffered saline) and TTBS (TBS with Tween 20) were used in Western blotting.

Antibodies

The fluorescein-labeled antibody B6H12-FITC was used against human CD47 (BD Biosciences). Opsonizing antibodies against human and sheep RBCs included rabbit anti–human RBCs, and rabbit anti–sheep RBCs (Sigma-Aldrich); these were used as IgG opsonin in phagocytosis assays. Antibodies against NMM IIA, actin was obtained from Sigma-Aldrich. Antibodies against streptavidin coated polystyrene beads (Spherotech) included rabbit anti-streptavidin (Sigma-Aldrich) and rabbit anti-streptavidin conjugated with FITC (Rockland Immunochemicals) used also as IgG opsonin in phagocytosis assays. Secondary antibodies used for detecting opsonin levels and uningested beads included goat anti–rabbit FITC or goat anti–rabbit F(ab')$_2$ R-PE (Sigma-Aldrich). Secondary antibodies used for detecting SIRPα binding included anti-GST Alexa 488 (Invitrogen). Antibodies against Syk (SYK-01) were purchased from AbCam, and Phospho-Syk (Tyr525/526), Phospho c-Cbl (Tyr774), and c-Cbl (2747) were purchased from Cell Signaling Technology.

Plasmid construction

The plasmid vector containing a cytomegalovirus promoter in pEGFP-C3 containing the DNA fragment encoding aa 1–1961 from NMHC II-A were obtained from Addgene. The original construct was prepared as described (Wei and Adelstein, 2000). To generate pCMV-GFP-ΔC170 encoding aa 1–1791, the original NMHC II-A construct from Addgene was digested with AflII–SpeI and the purified larger fragment was rendered blunt and self-ligated. pCMV-GFP-NMHC II-A point mutants Y277F and Y1805F were mutated by using primers 5′-CCTTCCACATCTTCTTTTATCTCCTGTCTGG-3′ and 5′-TCAAGTCCAAGTTCAAGGCCTCCATC-3′, respectively; done using the QuikChange Site-Directed Mutagenesis kit (Stratagene). For convenience pCMV-GFP-NMHC II-A, pCMV-GFP-ΔC170, and pCMV-GFP-NMHC II-A point mutants Y277F and Y1805F will be referred to as GFP-NMM II-A, GFP- ΔC170, GFP-Y277F, and GFP-Y1805F, respectively. All constructs were confirmed by sequencing.

Lentiviral knockdown of NMM IIA in THP-1 cells

ShRNA lentiviral supernatants to NMM IIA purchased from Sigma-Aldrich were targeting MYH9 (TRC#: TRCN0000029467) encoding NMM IIA. Further details of these clones are available from the Sigma-Aldrich website. Target THP-1 cells were infected with lentiviral supernatants at a multiplicity of infection (MOI) of 10, and then cells with integrated viral sequence were selected using puromycin (Sigma-Aldrich) at 2 μg/ml and then passaged with continuous puromycin selection. The degree of NMM IIA silencing was regularly monitored by both immunofluorescence and Western blotting. Control cell cultures were generated with control lentiviruses in parallel.

Cell culture and transfection

COS-1, CHO-K1, and THP-1 cells (American Type Culture Collection) were respectively maintained in DMEM, MEMα, and RPMI 1640 media (Invitrogen)—all supplemented with 10% FBS (Sigma-Aldrich). Differentiation of THP-1 cells was achieved in 100 ng/ml phorbol myristate acetate (PMA) (Sigma-Aldrich) for 2 d and confirmed by attachment of these cells to tissue-culture plastic. Peripheral blood monocytes from human donors were obtained through the Human Immunology Core (University of Pennsylvania, Philadelphia, PA). Human blood was obtained from finger pricks of healthy donors. Blood from other species was obtained from Covance and washed 3x in PBS plus 0.4% BSA. Sheep and human RBCs were used because of the different degrees of binding to human SIRPα at saturating levels with human RBCs having the highest interaction, and sheep RBCs at the lowest interaction as demonstrated by flow cytometry (Fig. 1 A).

GFP-NMHC II-A, GFP-ΔC170, and GFP-Y1805F were transfected into THP-1 wild-type cells with Effectene (QIAGEN) according to manufacturer's instructions. Clones resistant to 400 μg/ml G418 (Invitrogen) were selected. For clones with endogenous NMM IIA shRNA knockdown transfected with GFP-NMM II-A were resistant to both 400 μg/ml G418 and 2 μg/ml puromycin. The resulting resistant cells were maintained at 200 μg/ml.

Soluble human SIRPα production

COS-1 cells were transfected with pcDNA3-based vector (Seiffert et al., 1999) encoding a human SIRPα extracellular domain (variant: NA18949_V10) (Kharitonenkov et al., 1997) fused to GST using Lipofectamine 2000 (Invitrogen). Secreted SIRPα1-GST (referred to simply as hSIRPα) was affinity purified using Glutathione Sepharose 4B (Amersham Biosciences) and dialyzed against PBS (Invitrogen). The protein was stored at −20°C with or without addition of 10% (vol/vol) glycerol (Thermo Fisher Scientific).

Production of recombinant human CD47

Plasmids encoding the extracellular domain of human CD47 were PCR amplified, digested with XbaI and SalI (New England Biolabs, Inc.), and ligated to similarly digested vector, pEF-BOS-XB (Vernon-Wilson et al., 2000), which results in an in-frame fusion of CD4d3 + 4-biotin at the C terminus of the extracellular domain of CD47. The above vector containing the extracellular domain of CD47 was transfected into CHO (−K1) cells using Lipofectamine 2000 (Invitrogen). Secreted CD47-CD4d3 + 4 was concentrated using a 10 K MWCO Amicon (Millipore) and biotinylated at the C terminus using a biotin–protein ligase (Avidity, LLC) and dialyzed against PBS (Invitrogen). The protein was affinity purified using a monomeric avidin (Promega) and dialyzed against PBS (Invitrogen).

Preparation and quantification of CD47 density on polystyrene beads

Streptavidin-coated polystyrene beads of 2.1 μm diameter (Spherotech) were washed and blocked 3x in PBS plus 0.4% BSA. Biotinylated human CD47 was attached to streptavidin-coated beads at room temperature for 30 min, washed 3x, and resuspended in PBS plus 0.4% BSA.

The density of human CD47 present on the beads was labeled with saturating levels of B6H12-FITC and mIAP301-FITC (BD Biosciences), respectively for 30 min at room temperature. Beads were washed and resuspended in PBS/0.4% BSA and stored on ice until flow cytometric analysis. Mean fluorescence intensities were calibrated against uncoated streptavidin beads labeled with saturating B6H12-FITC/mIAP301-FITC levels (Fig. S2, E and F). The fluorescent intensities were standardized using Quantum FITC Molecule of Equivalent Soluble Fluorochrome (MESF) units (Bangs Laboratories). The MESF value for the human CD47 beads was then divided by the number of fluorophore per antibody to obtain the number of molecules per bead. The density of CD47 molecules on the streptavidin bead was determined for the bead by dividing the surface area (SA) of the 2.1-μm bead (SA = 13.9 μm^2). The density of CD47 molecules on human RBCs (SA = 128 μm^2) was also determined as described for the CD47 beads.

Binding isotherm for soluble hSIRPα for CD47 coated beads

Human CD47 was attached to the identical density as described above. The binding isotherm of soluble hSIRPα was performed for different species over a range of concentration using flow cytometry. Forward scatter, side scatter, and fluorescence (FL1, FL2, FL3, FL4 channels in logarithmic mode) were acquired for a least 10^4 events using a FACScan or FACSCalibur (BD Immunocytometry Systems). Data points from flow cytometry were plotted and fitted: the K_d values for human CD47-coated beads was 0.12 μM and 6.9 μM, respectively (Fig. 1 B).

Phagocytosis assay

For phagocytosis assays, macrophages were plated in 4-cm^2 Laboratory-Tek II chambered coverglass (Nalge Nunc International) at $10^5/cm^2$. Streptavidin polystyrene beads or RBCs were added to macrophages at a ratio of 20:1 and allowed to incubate at 37°C for 45 min. Non-phagocytosed beads or RBCs were washed with PBS. Cells were fixed with 5% formaldehyde (Thermo Fischer Scientific) for 5 min, followed by immediate replacement with PBS. For differentiation of non-internalized beads, beads were labeled with a primary antibody, rabbit anti-streptavidin (Sigma-Aldrich) at 1:1,000 in PBS for 20 min at 25°C. A second antibody, anti–rabbit R-PE (Sigma-Aldrich) was added at 1:1,000 in PBS to the cells and incubated for an additional 20 min at 25°C. Cells were then washed with PBS/0.4% BSA and then quantified by light and fluorescent microscopy. At least 200 cells were scored per well and experiments were repeated at least three times. Assays using RBCs as targets, lysis of uningested RBCs was performed by adding deionized H_2O for 60 s, followed by immediate replacement with PBS/0.4% BSA and fixing with 5% formaldehyde for 5 min.

For stimulated phagocytosis assays, beads with or without CD47 were incubated with rabbit anti-streptavidin serum and for sheep and human RBCs with rabbit anti–sheep RBCs and rabbit anti–human RBCs, respectively, as the opsonin. Beads or RBCs were opsonized at the respective concentration for 30 min at room temperature. In some experiments, human CD47 was blocked with a F(ab')$_2$ monoclonal antibody against CD47. The Fc fragments of mAb B6H12 were removed by Ficin digestion and separation by protein A chromatography after 10 min of the addition of opsonin. Opsonized beads and RBC were washed 2x and resuspended in 50 μl of PBS/0.4% BSA. Phagocytes were washed with PBS and uningested RBC was lysed and uningested beads were labeled as described above.

For cytoskeletal involvement at the phagocytic synapse, sheep and human RBCs were opsonized with rabbit anti–sheep RBCs or rabbit anti–human RBCs, respectively. Opsonized RBC cells were added to THP-1

cells, PMA treated, and immediately placed at 4°C for 30 min to synchronize phagocytosis. The temperature of the cells was then immediately increased to 37°C for 10 min and then fixed with 5% formaldehyde for immunofluorescence. For studies involving blebbistatin (EMD Biosciences), macrophages were treated for 10 min at 4°C before temperature increase to 37°C or for 45 min and 37°C. Macrophages treated with DMSO were used to verify no solvent effects.

Adhesion studies were done as above with incubations at 4°C for 30 min, and then the cultures were fixed and gently washed in PBS to eliminate non-adherent cells. RBCs per phagocyte were then counted.

Quantification of fluorescent intensity

Immunostaining was performed by permeabilization with 0.1% Triton X-100 in PBS for 20 min before blocking for 1 h with 5% BSA in PBS. Staining with primary antibodies was performed for 1 h at room temperature in PBS. After washing, samples were incubated with appropriate PE-conjugated secondary antibodies (1:1,000). To label cytoskeletal proteins at the phagocytic synapse, primary antibodies prepared with Zenon Alexa 488 or Zenon Alexa 647 Fab Labeling kits (Invitrogen) were labeled for 45 min at room temperature. Cells were immediately fixed using 5% formaldehyde for 20 min and washed with PBS. Samples were analyzed by differential interference contrast (DIC) and fluorescence microscopy.

Images were acquired with an inverted microscope (IX71; Olympus) with a 60x (oil, 1.4 NA) objective using a Cascade CCD camera (Photometrics). Image acquisition was performed with Image Pro software (Media Cybernetics, Inc.). Time-lapse imaging was performed using a heated stage (Ibidi GmbH) at 37°C in normal growth medium. Intensity analysis of the phagocytic synapse was performed using ImageJ with a 10 × 2 μm box. The synapse was aligned at the center of the 10-μm length box and the peak intensity designated as the zero in the distance scale on the plots. Fluorescence intensity was normalized by setting the cytoplasmic signal to 1 as the base signal, and five randomly selected cells were averaged. Two-tailed *t* tests were performed to assess the significance.

Immunoprecipitation and Western blotting

Human phagocytes, THP-1 cells (2×10^6) were cultured and differentiated in 6-well plates for 48 h after PMA differentiation. Human CD47 was attached to 2.1-μm beads at specific densities as described in the text and added at a bead-to-cell ratio of 20:1 for 2, 5, 10, and 30 min. After the incubation time, the cells were washed with ice-cold PBS and then lysed on ice in 400 μl of lysis buffer (50 mM Tris-HCl, pH 7.4, 150 mM NaCl, 1 mM EDTA, 1% NP-40, 1% protease inhibitor cocktail [Sigma-Aldrich], and 2 mM activated sodium orthovanadate). For immunoprecipitation, whole lysate was mixed with anti-SIRPα antibody conjugated to agarose (Santa Cruz Biotechnology, Inc.) at 4°C overnight. Precipitated proteins were separated on 10% SDS-PAGE (Invitrogen) and transferred to PVDF membrane for Western blotting, in which phosphotyrosine IgG HRP-conjugated and anti-SIRPα followed by IgG HRP-conjugated (Santa Cruz Biotechnology, Inc.) as primary antibodies. For Western blot, macrophage whole lysate or immunoprecipitated samples were separated on 4–12% SDS-PAGE and blotted onto PVDF membrane.

Online supplemental material

Fig. S1 shows the adhesion frequency of ShRBC and HuRBC. Fig. S2 shows the antibody and microbead characterization and demonstrates CD47 and IgG-opsonin noncompetitive binding; functional interaction of recombinant CD47 on beads. Fig. S3 shows that blebbistatin inhibits phagocytosis with an inhibition constant, $K^i \approx 5$ μM. Fig. S4 shows the expression of GFP-NMM IIA. Fig. S5 shows additional minor signaling differences in THP-1 lysates. Table S1 lists the proteins in THP-1 cell lysates identified via mass spectrometry in the different gel excised. Online supplemental material is available at http://www.jcb.org/cgi/content/full/jcb.200708043/DC1.

The authors gratefully acknowledge Dr. S. Subramanian for providing purified SIRPα.

Support of the National Institutes of Health and National Science Foundation is gratefully acknowledged.

Submitted: 6 August 2007
Accepted: 8 February 2008

References

Aderem, A., and D.M. Underhill. 1999. Mechanisms of phagocytosis in macrophages. *Annu. Rev. Immunol.* 17:593–623.

Allen, L.A., and A. Aderem. 1996. Molecular definition of distinct cytoskeletal structures involved in complement- and Fc receptor-mediated phagocytosis in macrophages. *J. Exp. Med.* 184:627–637.

Araki, N., M.T. Johnson, and J.A. Swanson. 1996. A role for phosphoinositide 3-kinase in the completion of macropinocytosis and phagocytosis by macrophages. *J. Cell Biol.* 135:1249–1260.

Arndt, P.A., and G. Garratty. 2004. Rh(null) red blood cells with reduced CD47 do not show increased interactions with peripheral blood monocytes. *Br. J. Haematol.* 125:412–414.

Baba, T., N. Fusaki, N. Shinya, A. Iwamatsu, and N. Hozumi. 2003. Myosin is an in vivo substrate of the protein tyrosine phosphatase (SHP-1) after mIgM cross-linking. *Biochem. Biophys. Res. Commun.* 304:67–72.

Beningo, K.A., and Y.-l. Wang. 2002. Fc-receptor-mediated phagocytosis is regulated by mechanical properties of the target. *J. Cell Sci.* 115:849–856.

Botelho, R.J., M. Teruel, R. Dierckman, R. Anderson, A. Wells, J.D. York, T. Meyer, and S. Grinstein. 2000. Localized biphasic changes in phosphatidylinositol-4,5-bisphosphate at sites of phagocytosis. *J. Cell Biol.* 151:1353–1368.

Brandt, D.T., S. Marion, G. Griffiths, T. Watanabe, K. Kaibuchi, and R. Grosse. 2007. Dia1 and IQGAP1 interact in cell migration and phagocytic cup formation. *J. Cell Biol.* 178:193–200.

Brown, E.J., and W.A. Frazier. 2001. Integrin-associated protein (CD47) and its ligands. *Trends Cell Biol.* 11:130–135.

Brown, M.H., and A.N. Barclay. 1994. Expression of immunoglobulin and scavenger receptor superfamily domains as chimeric proteins with domains 3 and 4 of CD4 for ligand analysis. *Protein Eng.* 7:515–521.

Brown, M.H., K. Boles, P.A. van der Merwe, V. Kumar, P.A. Mathew, and A.N. Barclay. 1998. 2B4, the natural killer and T cell immunoglobulin superfamily surface protein, is a ligand for CD48. *J. Exp. Med.* 188:2083–2090.

Cambier, J.C. 1995. Antigen and Fc receptor signaling. The awesome power of the immunoreceptor tyrosine-based activation motif (ITAM). *J. Immunol.* 155:3281–3285.

Caron, E., and A. Hall. 1998. Identification of two distinct mechanisms of phagocytosis controlled by different Rho GTPases. *Science.* 282:1717–1721.

Conti, M.A., and R.S. Adelstein. 2008. Nonmuscle myosin II moves in new directions. *J. Cell. Sci.* 121:11–18.

Conti, M.A., S. Even-Ram, C. Liu, K.M. Yamada, and R.S. Adelstein. 2004. Defects in cell adhesion and the visceral endoderm following ablation of nonmuscle myosin heavy chain II-A in mice. *J. Biol. Chem.* 279:41263–41266.

Cooney, D.S., H. Phee, A. Jacob, and K.M. Coggeshall. 2001. Signal transduction by human-restricted Fc gamma RIIa involves three distinct cytoplasmic kinase families leading to phagocytosis. *J. Immunol.* 167:844–854.

Coppolino, M.G., M. Krause, P. Hagendorff, D.A. Monner, W. Trimble, S. Grinstein, J. Wehland, and A.S. Sechi. 2001. Evidence for a molecular complex consisting of Fyb/SLAP, SLP-76, Nck, VASP and WASP that links the actin cytoskeleton to Fcgamma receptor signalling during phagocytosis. *J. Cell Sci.* 114:4307–4318.

Crowley, E., and A.F. Horwitz. 1995. Tyrosine phosphorylation and cytoskeletal tension regulate the release of fibroblast adhesions. *J. Cell Biol.* 131:525–537.

Crowley, M.T., P.S. Costello, C.J. Fitzer-Attas, M. Turner, F. Meng, C. Lowell, V.L. Tybulewicz, and A.L. DeFranco. 1997. A critical role for Syk in signal transduction and phagocytosis mediated by Fcgamma receptors on macrophages. *J. Exp. Med.* 186:1027–1039.

Dahl, K.N., R. Parthasarathy, C.M. Westhoff, D.M. Layton, and D.E. Discher. 2004. Protein 4.2 is critical to CD47-membrane skeleton attachment in human red cells. *Blood.* 103:1131–1136.

Diakonova, M., G. Bokoch, and J.A. Swanson. 2002. Dynamics of cytoskeletal proteins during Fcgamma receptor-mediated phagocytosis in macrophages. *Mol. Biol. Cell.* 13:402–411.

Duchemin, A.M., L.K. Ernst, and C.L. Anderson. 1994. Clustering of the high affinity Fc receptor for immunoglobulin G (Fc gamma RI) results in phosphorylation of its associated gamma-chain. *J. Biol. Chem.* 269:12111–12117.

Engler, A.J., S. Sen, H.L. Sweeney, and D.E. Discher. 2006. Matrix elasticity directs stem cell lineage specification. *Cell.* 126:677–689.

Fujioka, Y., T. Matozaki, T. Noguchi, A. Iwamatsu, T. Yamao, N. Takahashi, M. Tsuda, T. Takada, and M. Kasuga. 1996. A novel membrane glycoprotein, SHPS-1, that binds the SH2-domain-containing protein tyrosine phosphatase SHP-2 in response to mitogens and cell adhesion. *Mol. Cell. Biol.* 16:6887–6899.

Gardai, S.J., K.A. McPhillips, S.C. Frasch, W.J. Janssen, A. Starefeldt, J.E. Murphy-Ullrich, D.L. Bratton, P.-A. Oldenborg, M. Michalak, and P.M. Henson. 2005. Cell-surface calreticulin initiates clearance of viable or apoptotic cells through trans-activation of LRP on the phagocyte. *Cell.* 123:321–334.

Ghazizadeh, S., J.B. Bolen, and H.B. Fleit. 1994. Physical and functional association of Src-related protein tyrosine kinases with Fc gamma RII in monocytic THP-1 cells. *J. Biol. Chem.* 269:8878–8884.

Greenberg, S., K. Burridge, and S.C. Silverstein. 1990. Colocalization of F-actin and talin during Fc receptor-mediated phagocytosis in mouse macrophages. *J. Exp. Med.* 172:1853–1856.

Greenberg, S., J. el Khoury, F. di Virgilio, E.M. Kaplan, and S.C. Silverstein. 1991. Ca(2+)-independent F-actin assembly and disassembly during Fc receptor-mediated phagocytosis in mouse macrophages. *J. Cell Biol.* 113:757–767.

Greenberg, S., P. Chang, and S.C. Silverstein. 1994. Tyrosine phosphorylation of the gamma subunit of Fc gamma receptors, p72syk, and paxillin during Fc receptor-mediated phagocytosis in macrophages. *J. Biol. Chem.* 269:3897–3902.

Hall, A. 1998. Rho GTPases and the actin cytoskeleton. *Science.* 279:509–514.

Heath, K.E., A. Campos-Barros, A. Toren, G. Rozenfeld-Granot, L.E. Carlsson, J. Savige, J.C. Denison, M.C. Gregory, J.G. White, D.F. Barker, et al. 2001. Nonmuscle myosin heavy chain IIA mutations define a spectrum of autosomal dominant macrothrombocytopenias: May-Hegglin anomaly and Fechtner, Sebastian, Epstein, and Alport-like syndromes. *Am. J. Hum. Genet.* 69:1033–1045.

Huang, M.M., Z. Indik, L.F. Brass, J.A. Hoxie, A.D. Schreiber, and J.S. Brugge. 1992. Activation of Fc gamma RII induces tyrosine phosphorylation of multiple proteins including Fc gamma RII. *J. Biol. Chem.* 267:5467–5473.

Izaguirre, G., L. Aguirre, P. Ji, B. Aneskievich, and B. Haimovich. 1999. Tyrosine phosphorylation of alpha-actinin in activated platelets. *J. Biol. Chem.* 274:37012–37020.

Jiang, P., C.F. Lagenaur, and V. Narayanan. 1999. Integrin-associated protein is a ligand for the P84 neural adhesion molecule. *J. Biol. Chem.* 274:559–562.

Kant, A.M., P. De, X. Peng, T. Yi, D.J. Rawlings, J.S. Kim, and D.L. Durden. 2002. SHP-1 regulates Fcgamma receptor-mediated phagocytosis and the activation of RAC. *Blood.* 100:1852–1859.

Kharitonenkov, A., Z. Chen, I. Sures, H. Wang, J. Schilling, and A. Ullrich. 1997. A family of proteins that inhibit signalling through tyrosine kinase receptors. *Nature.* 386:181–186.

Kovacs, M., J. Toth, C. Hetenyi, A. Malnasi-Csizmadia, and J.R. Sellers. 2004. Mechanism of blebbistatin inhibition of myosin II. *J. Biol. Chem.* 279:35557–35563.

Kudryashov, D.S., A.V. Vorotnikov, T.V. Dudnakova, O.V. Stepanova, T.J. Lukas, J.R. Sellers, D.M. Watterson, and V.P. Shirinsky. 2002. Smooth muscle myosin filament assembly under control of a kinase-related protein (KRP) and caldesmon. *J. Muscle Res. Cell Motil.* 23:341–351.

Latour, S., H. Tanaka, C. Demeure, V. Mateo, M. Rubio, E.J. Brown, C. Maliszewski, F.P. Lindberg, A. Oldenborg, A. Ullrich, et al. 2001. Bidirectional negative regulation of human T and dendritic cells by CD47 and its cognate receptor signal-regulator protein-alpha: down-regulation of IL-12 responsiveness and inhibition of dendritic cell activation. *J. Immunol.* 167:2547–2554.

Limouze, J., A.F. Straight, T. Mitchison, and J.R. Sellers. 2004. Specificity of blebbistatin, an inhibitor of myosin II. *J. Muscle Res. Cell Motil.* 25:337–341.

Lowry, M.B., A.M. Duchemin, J.M. Robinson, and C.L. Anderson. 1998. Functional separation of pseudopod extension and particle internalization during Fc gamma receptor-mediated phagocytosis. *J. Exp. Med.* 187:161–176.

Mansfield, P.J., J.A. Shayman, and L.A. Boxer. 2000. Regulation of polymorphonuclear leukocyte phagocytosis by myosin light chain kinase after activation of mitogen-activated protein kinase. *Blood.* 95:2407–2412.

May, R.C., and L.M. Machesky. 2001. Phagocytosis and the actin cytoskeleton. *J. Cell Sci.* 114:1061–1077.

McLachlin, D.T., and B.T. Chait. 2001. Analysis of phosphorylated proteins and peptides by mass spectrometry. *Curr. Opin. Chem. Biol.* 5:591–602.

Meng, W., M. Numazaki, K. Takeuchi, Y. Uchibori, Y. Ando-Akatsuka, M. Tominaga, and T. Tominaga. 2004. DIP (mDia interacting protein) is a key molecule regulating Rho and Rac in a Src-dependent manner. *EMBO J.* 23:760–771.

Mouro-Chanteloup, I., J. Delaunay, P. Gane, V. Nicolas, M. Johansen, E.J. Brown, L.L. Peters, C.L. Van Kim, J.P. Cartron, and Y. Colin. 2003. Evidence that the red cell skeleton protein 4.2 interacts with the Rh membrane complex member CD47. *Blood.* 101:338–344.

Niewohner, J., I. Weber, M. Maniak, A. Muller-Taubenberger, and G. Gerisch. 1997. Talin-null cells of *Dictyostelium* are strongly defective in adhesion to particle and substrate surfaces and slightly impaired in cytokinesis. *J. Cell Biol.* 138:349–361.

Okazawa, H., S. Motegi, N. Ohyama, H. Ohnishi, T. Tomizawa, Y. Kaneko, P.A. Oldenborg, O. Ishikawa, and T. Matozaki. 2005. Negative regulation of phagocytosis in macrophages by the CD47-SHPS-1 system. *J. Immunol.* 174:2004–2011.

Olazabal, I.M., E. Caron, R.C. May, K. Schilling, D.A. Knecht, and L.M. Machesky. 2002. Rho-kinase and myosin-II control phagocytic cup formation during CR, but not Fc[gamma]R, phagocytosis. *Curr. Biol.* 12:1413–1418.

Oldenborg, P.A., A. Zheleznyak, Y.F. Fang, C.F. Lagenaur, H.D. Gresham, and F.P. Lindberg. 2000. Role of CD47 as a marker of self on red blood cells. *Science.* 288:2051–2054.

Ostap, E.M. 2002. 2,3-Butanedione monoxime (BDM) as a myosin inhibitor. *J. Muscle Res. Cell Motil.* 23:305–308.

Sampath, R., P.J. Gallagher, and F.M. Pavalko. 1998. Cytoskeletal interactions with the leukocyte integrin beta2 cytoplasmic tail. Activation-dependent regulation of associations with talin and alpha-actinin. *J. Biol. Chem.* 273:33588–33594.

Sato, M.K., M. Takahashi, and M. Yazawa. 2007. Two regions of the tail are necessary for the isoform-specific functions of nonmuscle myosin IIB. *Mol. Biol. Cell.* 18:1009–1017.

Seiffert, M., C. Cant, Z. Chen, I. Rappold, W. Brugger, L. Kanz, E.J. Brown, A. Ullrich, and H.J. Buhring. 1999. Human signal-regulatory protein is expressed on normal, but not on subsets of leukemic myeloid cells and mediates cellular adhesion involving its counterreceptor CD47. *Blood.* 94:3633–3643.

Stendahl, O.I., J.H. Hartwig, E.A. Brotschi, and T.P. Stossel. 1980. Distribution of actin-binding protein and myosin in macrophages during spreading and phagocytosis. *J. Cell Biol.* 84:215–224.

Straight, A.F., A. Cheung, J. Limouze, I. Chen, N.J. Westwood, J.R. Sellers, and T.J. Mitchison. 2003. Dissecting temporal and spatial control of cytokinesis with a myosin II Inhibitor. *Science.* 299:1743–1747.

Strzelecka, A., B. Pyrzynska, K. Kwiatkowska, and A. Sobota. 1997. Syk kinase, tyrosine-phosphorylated proteins and actin filaments accumulate at forming phagosomes during Fcgamma receptor-mediated phagocytosis. *Cell Motil. Cytoskeleton.* 38:287–296.

Subramanian, S., R. Tsai, S. Sen, K.N. Dahl, and D.E. Discher. 2006. Membrane mobility and clustering of Integrin Associated Protein (IAP, CD47)–Major differences between mouse and man and implications for signaling. *Blood Cells Mol. Dis.* 36:364–372.

Subramanian, S., E.T. Boder, and D.E. Discher. 2007. Phylogenetic divergence of CD47 interactions with human signal regulatory protein alpha reveals locus of species specificity. Implications for the binding site. *J. Biol. Chem.* 282:1805–1818.

Swanson, J.A., M.T. Johnson, K. Beningo, P. Post, M. Mooseker, and N. Araki. 1999. A contractile activity that closes phagosomes in macrophages. *J. Cell Sci.* 112:307–316.

Takenaka, K., T.K. Prasolava, J.C. Wang, S.M. Mortin-Toth, S. Khalouei, O.I. Gan, J.E. Dick, and J.S. Danska. 2007. Polymorphism in Sirpa modulates engraftment of human hematopoietic stem cells. *Nat. Immunol.* 8:1313–1323.

Titus, M.A. 1999. A class VII unconventional myosin is required for phagocytosis. *Curr. Biol.* 9:1297–1303.

Tsuda, M., T. Matozaki, K. Fukunaga, Y. Fujioka, A. Imamoto, T. Noguchi, T. Takada, T. Yamao, H. Takeda, F. Ochi, et al. 1998. Integrin-mediated tyrosine phosphorylation of SHPS-1 and its association with SHP-2. Roles of Fak and Src family kinases. *J. Biol. Chem.* 273:13223–13229.

Turner, C.E., F.M. Pavalko, and K. Burridge. 1989. The role of phosphorylation and limited proteolytic cleavage of talin and vinculin in the disruption of focal adhesion integrity. *J. Biol. Chem.* 264:11938–11944.

Turrini, F., F. Mannu, P. Arese, J. Yuan, and P.S. Low. 1993. Characterization of the autologous antibodies that opsonize erythrocytes with clustered integral membrane proteins. *Blood.* 81:3146–3152.

Valerius, N.H., O. Stendahl, J.H. Hartwig, and T.P. Stossel. 1981. Distribution of actin-binding protein and myosin in polymorphonuclear leukocytes during locomotion and phagocytosis. *Cell.* 24:195–202.

Veillette, A., E. Thibaudeau, and S. Latour. 1998. High expression of inhibitory receptor SHPS-1 and its association with protein-tyrosine phosphatase SHP-1 in macrophages. *J. Biol. Chem.* 273:22719–22728.

Vernon-Wilson, E.F., W.J. Kee, A.C. Willis, A.N. Barclay, D.L. Simmons, and M.H. Brown. 2000. CD47 is a ligand for rat macrophage membrane signal regulatory protein SIRP (OX41) and human SIRPalpha 1. *Eur. J. Immunol.* 30:2130–2137.

Wang, E., J. Michl, L.M. Pfeffer, S.C. Silverstein, and I. Tamm. 1984. Interferon suppresses pinocytosis but stimulates phagocytosis in mouse peritoneal macrophages: related changes in cytoskeletal organization. *J. Cell Biol.* 98:1328–1341.

Wei, Q., and R.S. Adelstein. 2000. Conditional expression of a truncated fragment of nonmuscle myosin II-A alters cell shape but not cytokinesis in HeLa cells. *Mol. Biol. Cell.* 11:3617–3627.